

# The *COP1* Ortholog *PPS* Regulates the Juvenile–Adult and Vegetative–Reproductive Phase Changes in Rice

Nobuhiro Tanaka,<sup>a</sup> Hironori Itoh,<sup>b</sup> Naoki Sentoku,<sup>b</sup> Mikiko Kojima,<sup>c</sup> Hitoshi Sakakibara,<sup>c</sup> Takeshi Izawa,<sup>b</sup> Jun-Ichi Itoh,<sup>a</sup> and Yasuo Nagato<sup>a,1</sup>

<sup>a</sup> Graduate School of Agricultural and Life Sciences, University of Tokyo, Tokyo 113-8657, Japan

<sup>b</sup> National Institute of Agrobiological Sciences, Tsukuba, Ibaraki 305-8602, Japan

<sup>c</sup> RIKEN Plant Science Center, Tsurumi, Yokohama 230-0045, Japan

Because plant reproductive development occurs only in adult plants, the juvenile-to-adult phase change is an indispensable part of the plant life cycle. We identified two allelic mutants, *peter pan syndrome-1* (*pps-1*) and *pps-2*, that prolong the juvenile phase in rice (*Oryza sativa*) and showed that rice *PPS* is an ortholog of *Arabidopsis thaliana* *CONSTITUTIVE PHOTOMORPHOGENIC1*. The *pps-1* mutant exhibits delayed expression of *miR156* and *miR172* and the suppression of GA biosynthetic genes, reducing the GA<sub>3</sub> content in this mutant. In spite of its prolonged juvenile phase, the *pps-1* mutant flowers early, and this is associated with derepression of *RAP1B* expression in *pps-1* plants independently of the *Hd1-Hd3a/RFT1* photoperiodic pathway. *PPS* is strongly expressed in the fourth and fifth leaves, suggesting that it regulates the onset of the adult phase downstream of *MOR11* and upstream of *miR156* and *miR172*. Its ability to regulate the vegetative phase change and the time of flowering suggests that rice *PPS* acquired novel functions during the evolution of rice/monocots.

## INTRODUCTION

The life cycle of higher plants has three mutually distinct developmental stages: the embryogenetic, vegetative, and reproductive stages. The vegetative stage can be further divided into the juvenile and adult phases, which are distinguished by many morphological and physiological differences both in woody plants, such as English ivy (*Hedera helix*) and *Eucalyptus occidentalis* (Poethig, 1990; Jaya et al., 2010), which exhibit obvious heteroblasty, and in herbaceous plants, which exhibit different morphological and physiological characteristics in the juvenile and adult phases (Lawson and Poethig, 1995; Telfer et al., 1997; Asai et al., 2002). Importantly, because plants can initiate reproductive growth under appropriate environmental conditions only during the adult phase (Simpson et al., 1999; Poethig, 2003), the juvenile-to-adult phase change (also known as the vegetative phase change) has a critical role in plant development. Although the mechanisms underlying the vegetative phase change remain largely unknown, recent studies using heterochronic mutants have revealed that microRNAs (miRNAs) play a significant role in the phase change.

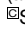
*Arabidopsis thaliana* rosette leaves are rounded with smooth leaf margins in the juvenile phase and are long, ovate, and serrated in the adult phase. The juvenile and adult leaves also

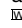
differ conspicuously in their patterns of trichome distribution; trichomes are found only on the adaxial side of juvenile leaves but are found on both sides of adult leaves (Telfer et al., 1997). These phenotypic markers have been used to identify *Arabidopsis* mutations causing a precocious phase change, many of which were subsequently associated with small RNAs. Mutations in *ZIPPY*, *SUPPRESSOR OF GENE SILENCING3*, and *RNA-DEPENDENT POLYMERASE6*, which are required for post-transcriptional silencing, are associated with the presence of trichomes on the abaxial sides of juvenile leaves (Hunter et al., 2003; Peragine et al., 2004). In the *squint* mutant, which forms abaxial trichomes on early leaves, the activity of *microRNA156* (*miR156*) is decreased because the ARGONAUTE1 protein is misfolded, resulting in the enhanced expression of the target genes, *SQUAMOSA PROMOTER BINDING PROTEIN-LIKE* (*SPL*) family genes encoding transcription factors (Smith et al., 2009). Ten of the 16 *SPL* genes in *Arabidopsis* are downregulated by *miR156b* (Schwab et al., 2005), and the *spl9* and *spl15* T-DNA insertion mutants exhibit prolonged juvenile phases (Schwarz et al., 2008). Conversely, overexpression of *SPL3/4/5* lacking the *miR156* target site causes a precocious phase change (Wu and Poethig, 2006). These findings indicate that small RNAs play an important role in the vegetative phase change in *Arabidopsis*.

In maize (*Zea mays*), juvenile leaves have epicuticular wax and no epidermal hair, and adult leaves have epidermal hair but no wax (Lawson and Poethig, 1995). As in *Arabidopsis*, miRNAs are involved in the vegetative phase change. The dominant *Corn-grass1* (*Cg1*) mutant encodes *miR156*, leading to overexpression of *miR156* and prolongation of the juvenile phase (Chuck et al., 2007). The *glossy15* (*gl15*) mutant shortens the juvenile phase in the maize epidermis (Moose and Sisco, 1994); *GL15* is an AP2-like gene harboring two AP2 domains (Moose and Sisco, 1996) that are targets of *miR172* (Lauter et al., 2005). In the early

<sup>1</sup> Address correspondence to anagato@mail.ecc.u-tokyo.ac.jp.

The author responsible for distribution of materials integral to the findings presented in this article in accordance with the policy described in the Instructions for Authors (www.plantcell.org) is: Yasuo Nagato (anagato@mail.ecc.u-tokyo.ac.jp).

 Some figures in this article are displayed in color online but in black and white in the print edition.

 Online version contains Web-only data.

www.plantcell.org/cgi/doi/10.1105/tpc.111.083436

vegetative stage, transcription of *miR156* far exceeds that of *miR172*, whereas later in the vegetative stage, the inverse pattern is seen: transcription of *miR172* far exceeds that of *miR156* (Lauter et al., 2005; Chuck et al., 2007). Inverse *miR156* and *miR172* expression patterns are also observed in *Arabidopsis* (Aukerman and Sakai, 2003; Wu and Poethig, 2006).

In a recent *Arabidopsis* study (Wu et al., 2009), *miR172* expression was shown to occur downstream of *SPL9* and *SPL10* expression, which is regulated by *miR156*. Thus, *miR156* and *miR172* may be key genes in the juvenile–adult phase change. The targets of *miR156* and *miR172* are known, but little is known about their upstream genes.

Gibberellin (GA) is a well-established regulatory phytohormone of the juvenile–adult phase change. In *Arabidopsis*, mutations in genes functioning in the biosynthesis of and response to GA prolong the juvenile phase (Telfer et al., 1997; Telfer and Poethig, 1998); the most severe mutation, *ga1-3*, causes the plant to fail to develop adult leaves (Telfer et al., 1997; Telfer and Poethig, 1998). Furthermore, GA treatment promotes the transition to adult phase in both *Arabidopsis* and maize (Evans and Poethig, 1995; Schwarz et al., 2008).

Although GA is known to promote the vegetative phase change, the other upstream and downstream factors controlling this phase change are largely unknown. However, because the juvenile–adult phase change affects a large number of traits, it is safe to assume that a large number of genes, including those encoding miRNAs, are involved in its regulation. A comprehensive understanding of the phase change will require the identification and functional characterization of more of the relevant genes.

To date, molecular genetic studies of the vegetative phase change have been concentrated mainly in two species, *Arabidopsis* and maize. However, rice (*Oryza sativa*) also has many morphological and physiological traits that differ between the juvenile and adult phases. These traits include the size of the shoot apical meristem (SAM), size and shape of leaf blades, presence or absence of midribs, vascular orientation in the stem, node–internode differentiation, and photosynthetic rate (Itoh et al., 2005). Only one mutation affecting the rice vegetative phase change, *mori1*, has been reported to date (Asai et al., 2002). Although this mutant has been characterized as perpetually maintaining the juvenile phase (Asai et al., 2002), the causal gene has not yet been cloned.

In this study, we attempted to identify additional rice mutants with altered vegetative phase changes. As a result, we isolated the *peter pan syndrome* (*pps*) mutant, which exhibits a prolonged juvenile phase and early flowering. Positional cloning revealed that *PPS* is an ortholog of *Arabidopsis* *CONSTITUTIVE PHOTOMORPHOGENIC1* (*COP1*).

## RESULTS

### Vegetative Phenotypes of *pps* Mutant

We identified one recessive rice mutant with a dwarf, dark-green phenotype (Figure 1A). The dwarf phenotype was maintained until the flowering stage. Because a detailed examination of the

juvenile/adult marker traits (described below) of this mutant revealed that it has a prolonged juvenile phase, we named this mutant *peter pan syndrome-1* (*pps-1*). Subsequently, we identified an additional allelic mutant, *pps-2*, that exhibited an even more severe mutant phenotype. Most *pps-2* seeds could not germinate, and only ~5% of seeds could germinate on nutrient medium containing sucrose but died in a week (Figure 1B). Thus, our analyses were performed primarily on *pps-1*.

Of the considerable number of morphological and physiological traits known to differ between the juvenile and adult phases in rice (Itoh et al., 2005), we first examined leaf shape. We observed that the ratio of leaf blade length to width rapidly increases with elevation of leaf position (Figure 1C); the leaf-blade length:width ratio for the second leaf blade is ~10:1, whereas that of the fifth leaf blade, which is much more slender, is greater than 50:1. By contrast, no rapid increase of the length:width ratio with elevation of leaf position was observed in the *pps-1* mutant; the ratio of even the eighth leaf blade of the mutant was comparable to that of the third leaf of wild-type plants (Figure 1C).

We also examined the leaf blades of the *pps-1* mutant for the presence of a midrib, which is normally seen in adult leaves. In wild-type plants, midribs were rarely observed in second leaves (Figure 1D). In third and fourth leaves, midribs were observed to cover approximately one-half of the total length from leaf base to leaf tip (~40 and 60% of the total length, respectively; Figures 1E and 1I). In the higher leaves, midribs covered at least 75% of the length of the blade (Figure 1I). By contrast, second, third, and fourth *pps-1* leaves exhibited almost no midrib (Figures 1F and 1I), and midrib formation in fifth leaf was ~20% of the total length (Figures 1G and 1I). Even in the sixth *pps-1* leaf, midrib length was comparable to that of a wild-type third leaf (Figures 1H and 1I). Thus, second to fourth *pps-1* leaves are structurally similar to wild-type second leaves, and fifth to sixth *pps-1* leaves are comparable to wild-type third leaves. This suggests that the *pps-1* sixth leaf is intermediate between juvenile and adult, suggesting that *pps-1* has more juvenile leaves.

An examination of other morphological traits supported this characterization of the *pps-1* mutant. Normally, SAMs enlarge gradually during development (Figure 1J), but the *pps-1* SAM remained unchanged in size until at least the fifth-leaf stage (Figure 1J). Furthermore, the *pps-1* mutant displayed different node–internode differentiation characteristics. Normally, below the insertion of the fourth leaf, the vascular bundles are irregular in orientation, and no node–internode differentiation is evident, whereas above the fourth leaf, the stem has obvious nodes (Figure 1K); in the mutant, on the other hand, the vascular orientation remained irregular up to the sixth leaf insertion, and no node differentiation was observable on the stem until the insertion of the seventh leaf (Figure 1L). Therefore, the stem structure of the *pps-1* mutant becomes adult above the sixth or seventh leaf insertion and is also consistent with a prolonged juvenile phase.

The physiological traits associated with the phase change in the *pps-1* mutant were also consistent with a prolonged juvenile phase. For example, in wild-type rice plants, photosynthesis is reduced in juvenile leaves (second leaves) and much more quickly in fourth and higher leaves (Figure 1M). By contrast, photosynthesis occurred slowly even in the fourth through eighth

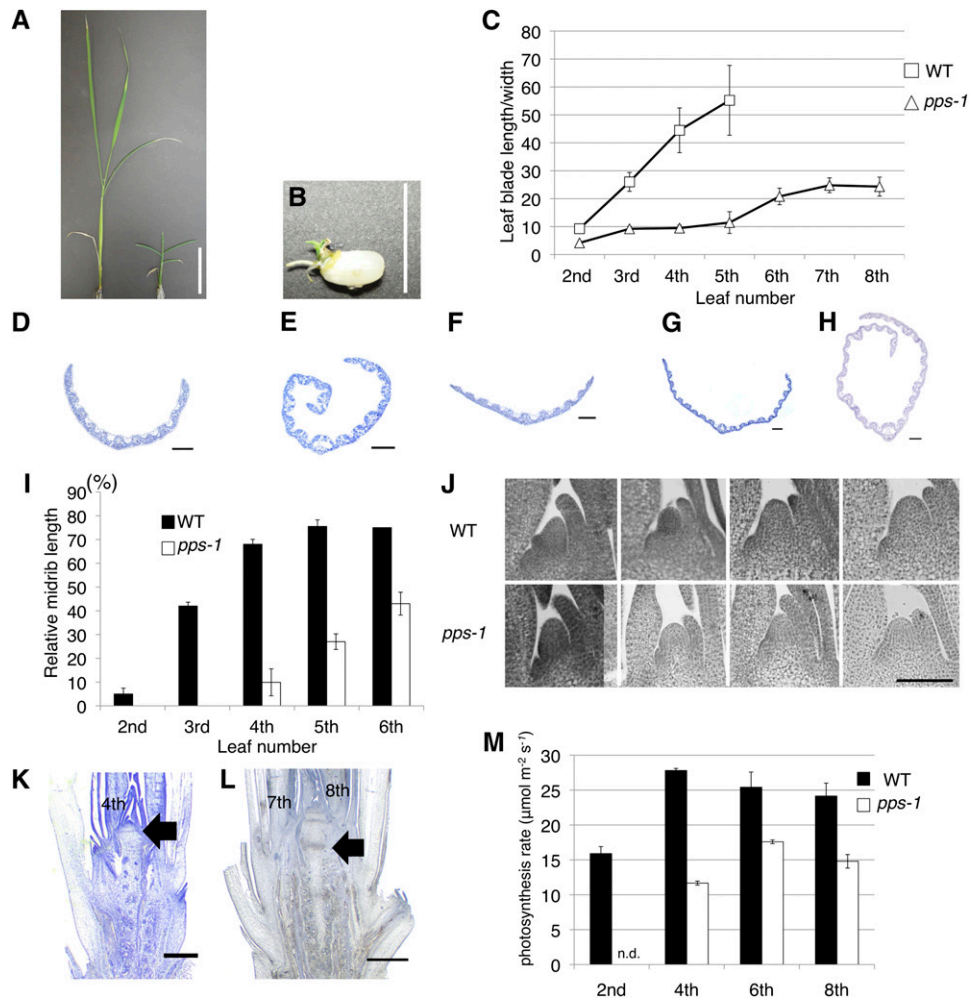


**Figure 1.** Phenotypes of *pps-1* Plants.

(A) Seedlings of 1-week-old wild type (left) and 1-week-old *pps-1* (right).

(B) A rare germinated *pps-2* seed.

(C) Comparison of the ratio of leaf blade length to width in the wild type (WT) versus *pps-1*.

(D) to (H) Cross sections of leaf blades.

(D) Cross section of wild-type second leaf blade cut at 10% of the distance from the base to the tip.

(E) Cross section of wild-type third leaf blade cut at 45% from the base.

(F) Cross section of *pps-1* fourth leaf blade cut at 10% from the base.

(G) Cross section of *pps-1* fifth leaf blade cut at 30% from the base.

(H) Cross section of *pps-1* sixth leaf blade cut at 40% from the base.

(I) Comparison of relative midrib length in leaf blades during development in the wild type versus *pps-1*. Midrib length is shown as a percentage of total blade length.

(J) Wild-type and *pps-1* shoot apices showing temporal change of SAM size. From left to right, second leaf stage, third leaf stage, fourth leaf stage, and fifth leaf stage.

(K) Fourteen-day-old wild-type stem. Arrow indicates fourth leaf base node.

(L) Thirty-day-old *pps-1* stem. Arrow indicates seventh leaf base node.

(M) Comparison of photosynthetic rates in the wild type and *pps-1*. Units =  $\mu\text{mol CO}_2 \text{ m}^{-2} \text{ s}^{-1}$ .

Data represent mean  $\pm$  SD in (C) and (I) ( $n = 5$ ) and in (M) ( $n = 3$ ). Bars = 1 cm in (A), 5 cm in (B), 100  $\mu\text{m}$  in (D) to (H), (K), and (L), and 50  $\mu\text{m}$  in (J).

[See online article for color version of this figure.]

leaves of the *pps-1* mutant; the rate was comparable to that in wild-type second leaves (Figure 1M). Thus, both morphological and physiological characteristics indicate that the juvenile phase extends to the sixth or eighth leaf in *pps-1* plants. In addition, adult *pps-1* plants were not normal (small stature and incomplete midrib formation). Thus, even in the late vegetative phase, juvenile characters coexist with adult characters.

### Profile of *miR156* and *miR172* Expression

When we used real-time PCR to examine *miR156* and *miR172* expression in wild-type plants, we found that the level of *miR156* expression was high in second leaves, but it decreased to less than half of this level in third leaves (Figure 2A). This low-level expression of *miR156* was maintained through the seventh leaf (Figure 2A). The *miR172* expression pattern was the inverse of that of *miR156*, as expected; the second and third leaves contained very little *miR172* transcripts, and the amount of *miR172* transcripts increased rapidly going up the stem to the seventh leaf (Figure 2B). Thus, expression of the *miR156* and *miR172* genes in wild-type rice is phase dependent and inversely regulated, as it is in maize and *Arabidopsis*.

In the *pps-1* mutant, the *miR156* expression level in third and fourth leaves was slightly lower than that in the second leaf but significantly higher than that in wild-type third and fourth leaves (Figure 2A). The *miR156* expression levels in the *pps-1* and wild-type plants did not become comparable until the sixth or seventh leaves (Figure 2A), indicating that *pps-1* delays the downregulation of *miR156* expression with elevation by two or three leaves. In addition, *miR172* expression levels in the *pps-1* mutant increased very slowly with development, so that the level in seventh *pps-1* leaves was only 20% of that in wild-type seventh leaves (Figure 2B). This result is also consistent with a delay in the juvenile–adult phase change. Thus, the *pps-1* mutation both affects the expression of *miR156* and *miR172* and prolongs the juvenile phase, providing strong evidence that *miR156* and *miR172* regulate the phase change downstream of *PPS* and that *PPS* promotes the transition to adult phase.

### Flowering Time

Notably, when about 10 leaves were formed, *pps-1* plants flowered ~3 weeks early under field conditions despite their prolonged juvenile period (Figures 3A and 3B), and the early flowering was independent of daylength (Figure 3B). Thus, *PPS* appears not only to promote the juvenile–adult phase change but also to suppress the transition from vegetative to reproductive stage.

To examine the mechanism of early flowering in *pps-1* plants, we first analyzed the expression of two florigen genes, *Hd3a* and *RFT1*, in plants with emerging sixth leaves. At this stage in typical photoperiodic cultivars of rice, the expression of the *Hd3a* and *RFT1* genes in leaves is critically controlled by photoperiods (Itoh et al., 2010). In Taichung 65, the background cultivar of *pps* and the *pps* mutants, two major rice flowering-time genes, *Hd1* (*Heading date 1*, a rice ortholog of *Arabidopsis CO*) and *Ehd1* (*Early heading date 1*), were mutated (Doi et al., 2004). Therefore, expressions of these genes were only slightly induced in the sixth leaves of Taichung 65 plants under short-day conditions and completely suppressed under long-day conditions (Doi et al., 2004). Although we expected to see enhanced expressions of the florigen genes in *pps-1* sixth leaves, they were completely suppressed (Figures 3C to 3F). This finding indicates that early flowering in *pps-1* plants is not caused by precocious activation of the *Hd1-Ehd1-Hd3a/RFT* photoperiodic pathway.

Since the *cop1* mutant exhibits a circadian clock phenotype (Millar et al., 1995), we further examined the diurnal expression of major circadian clock-related genes in rice (see Supplemental Figure 1 online). The results indicate that the amplitudes of *Os GI* and *Os PRR1* in *pps-1* were slightly reduced, but no critical changes were observed on phase setting of these genes. Similarly, no clear change was detected in *Os LHY* expression under short-day conditions. Together with the defects of *Hd1* and *Ehd1* in Taichung 65, which functions downstream of circadian clocks, it is unlikely that the early flowering phenotype of *pps* is caused by some defects in rice circadian clocks.

We next examined the expression of *RAP1B/Os MADS14*, which normally functions downstream of *Hd3a/RFT1* in the

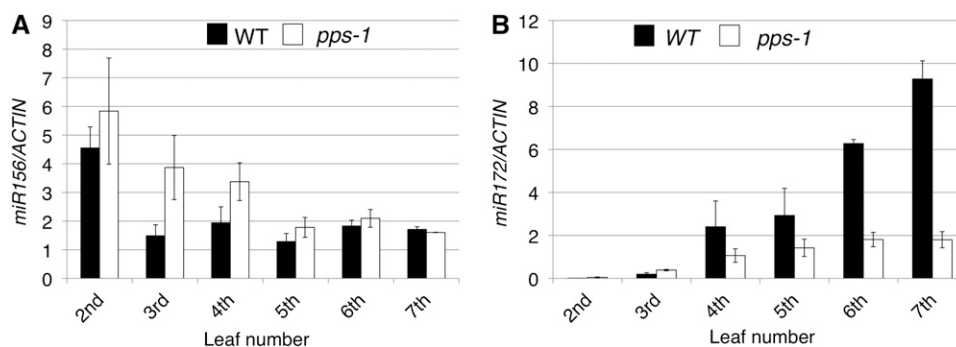


**Figure 2.** Expression of Two miRNAs in Wild-Type and *pps-1* Leaves.

(A) Expression of *miR156* in the second to seventh leaf blades. WT, wild type.

(B) Expression of *miR172* in the second to seventh leaf blades. Expression levels are represented relative to *ACTIN* expression. Each value is the average of three independent real-time PCR assays.

Data in (A) and (B) represent means  $\pm$  SD ( $n = 3$ ).

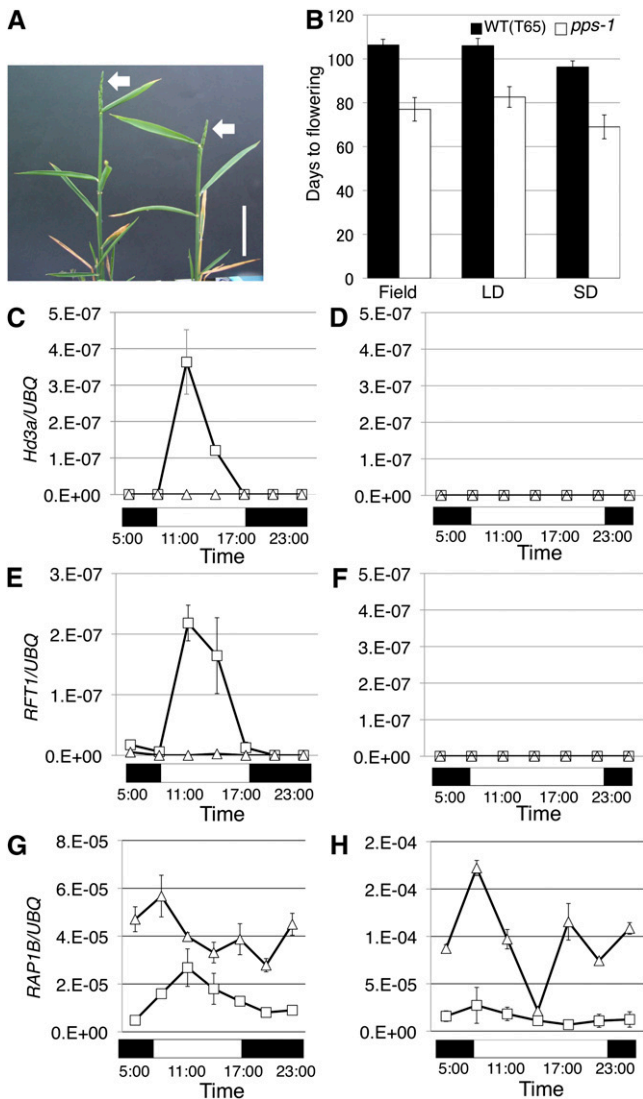


**Figure 3.** Early Flowering Phenotypes in *pps-1*.

(A) Mature *pps-1* plants. Arrows indicate panicles. Bar = 5 cm.  
 (B) Days to flowering in the wild type (WT) and *pps-1* in field conditions, long day (LD) and short day (SD).  
 (C) *Hd3a* expression under short-day conditions.  
 (D) *Hd3a* expression under long-day conditions.  
 (E) *RFT1* expression under short-day conditions.  
 (F) *RFT1* expression under long-day conditions.  
 (G) *RAP1B* expression under long-day conditions.  
 (H) *RAP1B* expression under short-day conditions.  
 (C) to (H) White squares, the wild type; white triangles, *pps-1*. Black and white boxes under each panel represent periods of darkness and light, respectively. Data represent mean  $\pm$  SD in (B) ( $n = 5$ ) and in (C) to (H) ( $n = 3$ ). [See online article for color version of this figure.]

positive regulation of floral homeotic genes (Komiya et al., 2008). *RAP1B* expression was higher in *pps-1* plants than in wild-type plants under both short-day and long-day conditions (Figures 3G and 3H). Thus, the early flowering in *pps-1* might result from derepression of *RAP1B*, independently of the *Hd3a/RFT1*-

mediated pathway. It is noted that overexpression of *RAP1B* caused a drastic early flowering (Jeon et al., 2000).

### GA-Related Phenotypes

To confirm that GA promotes the juvenile–adult phase change in rice, as it does in *Arabidopsis* and maize (Evans and Poethig, 1995; Telfer et al., 1997; Telfer and Poethig, 1998), we treated wild-type plants with either GA<sub>3</sub> or uniconazole, an inhibitor of GA biosynthesis. In addition to promoting rice plant growth (Figure 4A), as expected, GA<sub>3</sub> treatment also induced midrib formation in the second leaf blades (Figure 4B). Uniconazole treatment suppressed both of these processes (Figures 4A and 4B). In addition, examination of the GA-deficient dwarf mutant *d18-dy*, which has a defect in the gene encoding GA3 OXIDASE2, revealed suppression of midrib formation in the third and fourth leaf blades (Figure 4C), consistent with a prolonged juvenile phase. These findings indicate that GA promotes the juvenile–adult phase change in rice.

Treatment of *pps-1* plants with GA<sub>3</sub> or uniconazole had effects that were similar to those seen in wild-type plants (Figures 4A and 4B), establishing that *pps-1* plants have a normal sensitivity to GA. However, measurements of the amounts of active GA, GA<sub>1</sub>, and the intermediates GA<sub>53</sub>, GA<sub>44</sub>, GA<sub>19</sub>, and GA<sub>20</sub> revealed a significant reduction in the levels of all of these species in *pps-1* plants (Figure 4D). To determine the reason for the decreased GA content in *pps-1* plants, we compared the expression of genes encoding GA metabolizing enzymes in *pps-1* versus wild-type plants. Relative to the wild-type plants, the mutant plants expressed more *GA2 OXIDASE4*, which encodes a GA-catabolizing enzyme, with lower expression levels of *GA3 OXIDASE2* and *GA20 OXIDASE2*, which encode enzymes involved in GA biosynthesis (Figure 4E). Accordingly, the low GA content in *pps-1* plants appears to be caused by enhanced catabolism and suppressed anabolism of GA, indicating that *PPS* regulates the vegetative phase change upstream of GA.

### Positional Cloning of the *PPS* Gene

We identified the gene mutated in *pps-1* using a map-based approach with the F2 and F3 hybrids of *pps-1* heterozygotes and cv Kasalath (ssp *indica*). The *PPS* locus was mapped to  $\sim$ 139.5 centimorgans on the long arm of chromosome 2. This region of chromosome 2 harbors a putative *Arabidopsis COP1* ortholog, Os02g53140.1 (Tsuge et al., 2001). Sequencing of the ortholog revealed mutations in this gene for both *pps-1* and *pps-2*. The *pps-1* mutation consists of a single base change (G  $\rightarrow$  A) at the splicing acceptor site of the sixth exon of Os02g53140.1 on BAC clone OJ1353\_F08. The *pps-2* mutation consists of a single base change (G  $\rightarrow$  A) in the eighth exon of the gene, generating a premature stop codon in the same gene (Figure 5A). In *pps-1* plants, two types of *COP1* ortholog transcripts were found; one of these transcripts contained an inserted intron, and the other lacked nine conserved amino acids in the sixth exon, the former being a little more abundant than the latter (see Supplemental Figure 2 online). Consistent with the mutant phenotypes, we presumed that *pps-1* is a weaker allele than *pps-2*. Transformation of *pps-1* plants with Os02g53140.1 cDNA under control

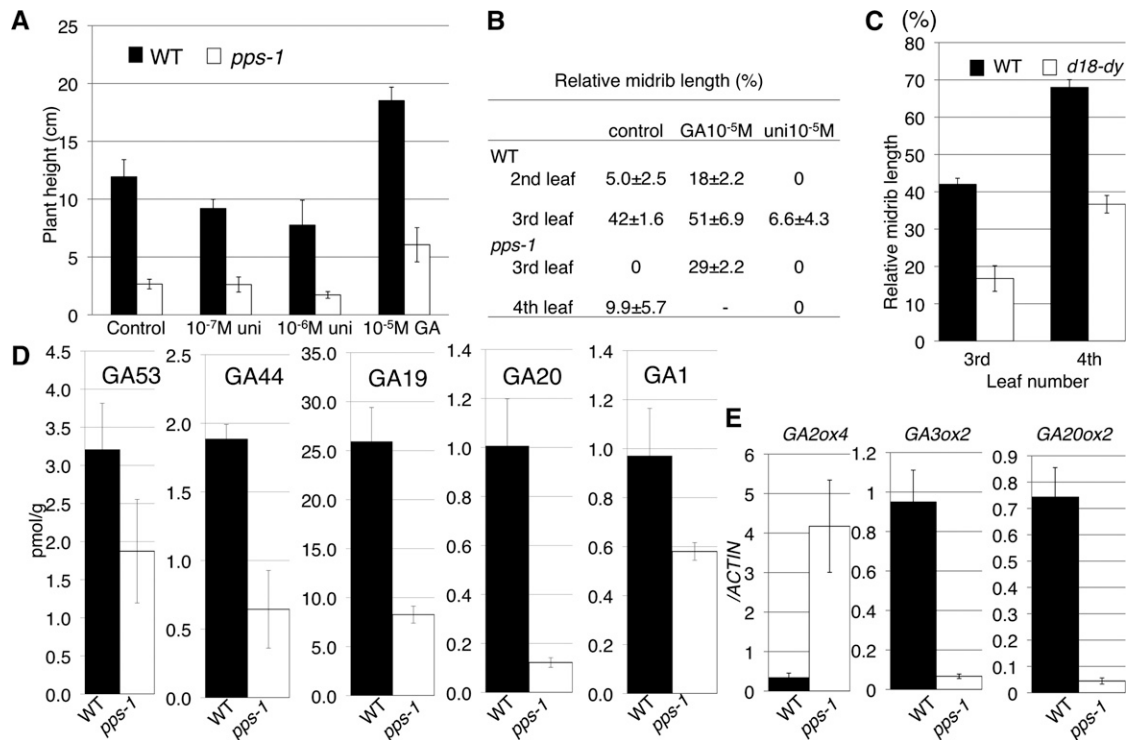


**Figure 4.** GA-Related Phenotypes in *pps-1*.

**(A)** Plant height of 1-week-old wild type (WT) and *pps-1* germinated on medium containing GA<sub>3</sub> or uniconazole.

**(B)** Relative length of midrib in the wild type and *pps-1* germinated on medium containing GA<sub>3</sub> or uniconazole. The values are shown as mean ± SD (*n* = 5).

**(C)** Relative length of midrib in third and fourth leaves of the wild type and *d18-dy*.

**(D)** Contents of GA<sub>53</sub>, GA<sub>44</sub>, GA<sub>19</sub>, GA<sub>20</sub>, and GA<sub>1</sub> in 3-week-old wild-type and *pps-1* seedlings.

**(E)** Real-time PCR analysis of GA metabolic gene expression in fourth leaves of the wild type and *pps-1*. Data represent mean ± SD in **(A)** to **(C)** (*n* = 5) and in **(D)** and **(E)** (*n* = 3).

of the *ACTIN* promoter restored the normal phenotype (see Supplemental Figure 3 online). We therefore concluded that Os02g53140.1 is the *PPS* gene.

The *PPS* gene is composed of 13 exons comprising 2058 nucleotides encoding a 685-amino acid polypeptide (Figure 5A). Os02g53140.1 is known to be an ortholog of *Arabidopsis COP1* (Tsuge et al., 2001). The PPS/COP1 protein includes three well-conserved domains (ring-finger, coiled-coil, and WD-40 repeat domains) that play roles in protein-protein interactions (Figure 5A). The amino acid sequences of PPS and COP1 are 73% identical.

### Pattern of *PPS* Expression

Rice *PPS* was previously reported (as a *COP1* ortholog) to be expressed in almost all tissues, including roots, calli, and leaves (Tsuge et al., 2001). In an RT-PCR analysis, we found low-level expression of *PPS* in shoot apices and young panicles (see Supplemental Figure 4 online). To elucidate the developmental regulation of *PPS* expression in leaves, we used real-time PCR to measure *PPS* mRNA levels in the second through eighth leaf blades. Expression of *PPS* was minimal in second leaves, began

to increase in third leaves, reached a peak in fourth and fifth leaves, and declined in higher leaves (Figure 5B). Since the rice juvenile phase is limited to the second leaf, and the juvenile-adult transition occurs in the third to fifth leaves, this expression pattern indicates that *PPS* is expressed primarily during the transition stage. This expression pattern also provides a straightforward explanation for the delayed adult phase initiation phenotype of *pps-1* (i.e., *PPS* is involved in the initiation of the phase transition). Consistent with the hypothesis that leaves play a major role in the phase change, the amount of *PPS* mRNA found in leaves of wild-type plants far exceeded that found in the shoot apices, including the SAMs and a few leaf primordia (Figure 5B).

The *mori1* mutant is the only heterochronic rice mutant reported to date with a perpetual juvenile phase (Asai et al., 2002), suggesting that *MORI1* is a master switch for the juvenile-adult phase change in rice. To examine the functional relationship between *MORI1* and *PPS*, we constructed a *mori1 pps-1* double mutant. This mutant exhibited a *mori1* phenotype (data not shown), showing that *MORI1* is epistatic to *PPS*. When we examined *PPS* expression in the *mori1* mutant background, we found that *PPS* expression was completely suppressed (Figure 5B), indicating that *MORI1* positively regulates *PPS* expression.

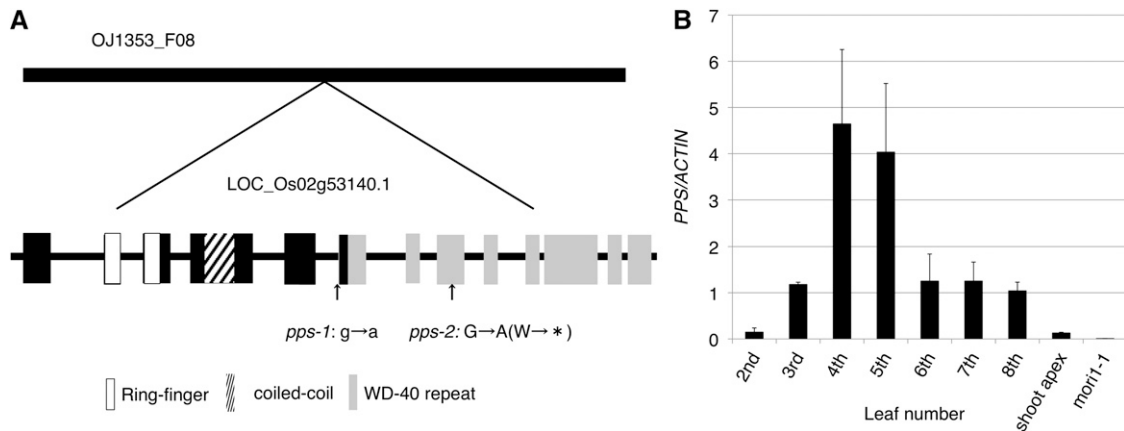


**Figure 5.** Molecular Characterization of the *PPS* Gene.

**(A)** *PPS* gene structure. White boxes, RING-FINGER domain; slanted line box, coiled-coil domain; gray box, WD-40 repeat. Mutation sites of two *pps* alleles are indicated by vertical arrows.

**(B)** Expression pattern of *PPS* (relative to *ACTIN-1*) in second to eighth wild-type leaf blades, 2-week-old wild-type shoot apex, and *mori1-1* seedling. Data represent means  $\pm$  SD ( $n = 3$ ).

### Comparison of *pps-1* and *cop1* Phenotypes

Because the *Arabidopsis cop1* mutant exhibits photomorphogenesis in the dark, we expected the *pps-1* mutant to also exhibit photomorphogenesis in the dark. Indeed, when we grew wild-type and *pps-1* plants in dark conditions, the wild-type plants were etiolated and showed active internode elongation, whereas internode elongation was suppressed in the *pps-1* plants, which were yellow (Figure 6A). In addition, the light-inducible *CHLOROPHYLL A/B BINDING PROTEIN (CAB)* gene was strongly expressed in dark-grown *pps-1* plants but almost completely suppressed in the dark-grown wild-type plants (Figure 6B). These results indicate that *PPS* is functionally equivalent to *COP1* in photomorphogenesis/scotomorphogenesis.

To investigate the effect of the *cop1* mutation on the vegetative phase change in *Arabidopsis* that has not been previously reported, we examined trichome distribution in early leaves of *Arabidopsis* plants harboring *cop1-4*, a weak allele that allows development through the reproductive stage. The number of the leaf on which abaxial trichomes first appeared was the same in wild-type and *cop1-4* plants (Figures 7A and 7B). In addition, expression levels of *miR156* and *miR172* genes in 10-d-old *cop1-4* seedling were comparable with those of the wild type (Figures 7C and 7D). Thus, *COP1*, unlike *PPS*, is not involved in the juvenile–adult phase change.

### DISCUSSION

Our analyses indicated that the *PPS* gene temporally regulates the onset of the adult phase, acting downstream of *MOR11* and upstream of miRNAs and GA-related genes. In addition, the *pps-1* mutant flowered early possibly due to precocious activation of *RAP1B*, independently of the *Hd3a/RFT* pathway. Positional cloning revealed that *PPS* is an ortholog of *Arabidopsis COP1*. Like the *cop1 Arabidopsis* mutant, the *pps-1* rice mutant ex-

hibited photomorphogenesis in the dark. Thus, *PPS* appears to have acquired novel functions associated with phase change regulation during the evolution of rice/monocots, as *COP1* does not appear to regulate the vegetative phase change or the time of flowering.

Our findings suggest that *PPS* promotes the juvenile–adult phase change in rice by regulating the expression of *miR156*, *miR172*, and GA-related genes. In maize, the dominant *Cg1* mutant exhibits a prolonged juvenile phase that results from overexpression of *miR156* (Chuck et al., 2007), and the *glossy15* mutant exhibits a shortened juvenile phase that results from a deficiency in the AP2 domain–containing gene target of *miR172*. In *Arabidopsis*, *miR156* and *miR172* have been reported to regulate the juvenile–adult phase change (Wu and Poethig, 2006; Schwarz et al., 2008; Wu et al., 2009). We found that the rice

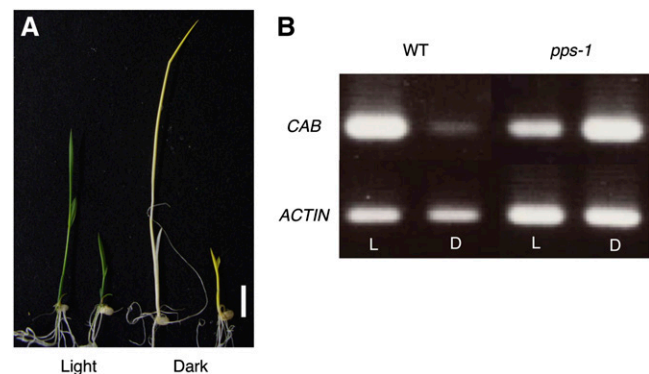


**Figure 6.** Photomorphogenesis of *pps-1* in the Dark.

**(A)** Seedlings grown in the light or in the dark. From left to right, 7-d-old wild type in the light, 7-d-old *pps-1* in the light, 7-d-old wild type in the dark, and 7-d-old *pps-1* in the dark. Bar = 1 cm.

**(B)** Expression of the *CAB* gene in the light (L) and dark (D). WT, wild type.

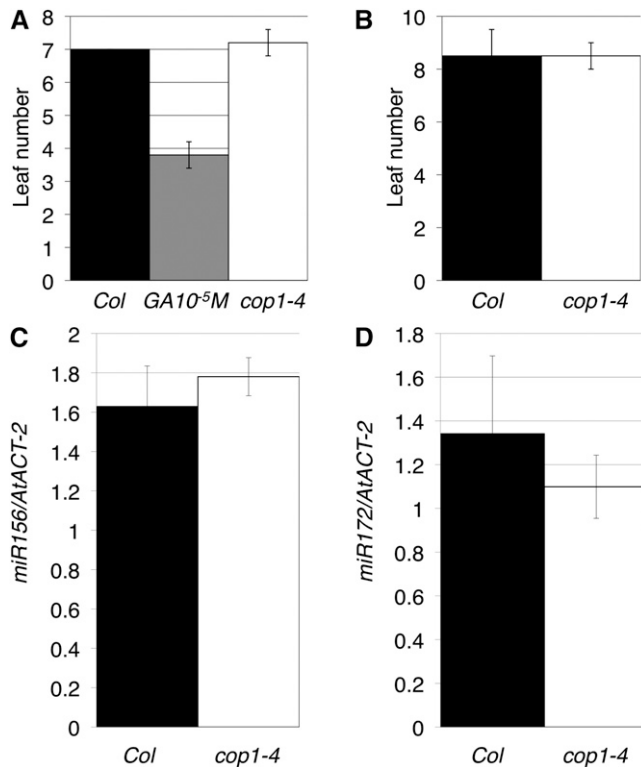


**Figure 7.** Vegetative Phase Change in *Arabidopsis cop1-4*.

(A) and (B) The leaf number on which abaxial trichomes first appeared in Columbia (Col), Col treated with  $10^{-5}$  M GA<sub>3</sub>, and *cop1-4* under long-day (A) and short-day (B) conditions.

(C) Real-time PCR analysis of *miR156* in 10-d-old Columbia and *cop1-4* seedlings.

(D) Real-time PCR analysis of *miR172* in 10-d-old Columbia and *cop1-4* seedlings.

Data represent mean  $\pm$  SD ( $n = 3$ ).

*pps-1* mutant exhibits a temporal delay in the downregulation of *miR156* expression and the upregulation of *miR172* expression during development. Thus, *miR156* and *miR172* might be ubiquitous regulators of the vegetative phase change in plants.

To comprehensively understand the genetic network regulating the juvenile–adult phase change, we must know which genes act upstream or downstream of *miR156* and *miR172*. Maize *GL15*, which is a target of *miR172* as described above, is exclusively associated with leaf epidermal identity (Moose and Sisco, 1994, 1996). On the other hand, there have been no reports of heterochronic gene(s) acting upstream of these miRNAs or of GA, although such genes would be expected to affect more traits than the miRNAs. Since *PPS* affects the expression of *miR156*, *miR172*, and GA metabolic genes and alters the temporal characteristics of a large number of traits, *PPS* appears to be positioned upstream of *miR156* and *miR172*. *mori1* is the first heterochronic rice mutant that remains perpetually in the juvenile phase and never flowers (Asai et al., 2002). On the other hand, *pps-1* exhibits adult characters later and flowers. These phenotypic differences imply that *PPS* is downstream of *MORI1*. In fact, *PPS* is not expressed in *mori1* mutants, suggesting that *MORI1* is

a master switch for the juvenile–adult phase change. Since many of the same traits are affected by the *mori1* and *pps* mutations, *PPS* probably integrates genes acting immediately or almost immediately downstream of *MORI1* (Figure 8).

Our results also suggest that *PPS* regulates the biosynthesis of GA in rice and that GA promotes the vegetative phase change in rice, as it does in *Arabidopsis* and maize (Evans and Poethig, 1995; Telfer et al., 1997), by promoting the transition to adult phase. GA<sub>1</sub> and the other intermediates of the GA biosynthetic pathway were present in lower concentrations in *pps-1* plants than in wild-type plants. Additionally, GA catabolic and biosynthetic genes were significantly upregulated and downregulated, respectively, in *pps-1* plants. These findings show that *PPS* is a positive regulator of GA synthesis.

Although close links between GA and photomorphogenesis have been demonstrated in *Arabidopsis* (Alabadi et al., 2008), whether *COP1* directly regulates GA biosynthesis has not been established. *LIP1*, a pea (*Pisum sativum*) ortholog of *COP1*, was recently reported to positively regulate GA biosynthesis through negative regulation of *LONG1*, an ortholog of the *COP1* target *HY5*, which negatively regulates GA biosynthesis (Weller et al., 2009). This case is comparable with that of *PPS*. Although the details of the mechanism by which *PPS* regulates GA biosynthesis remain to be determined, *PPS* acts upstream of GA metabolic genes, and the pleiotropic phenotypes in *pps-1* plants can be at least partially explained by GA deficiency.

The decreased GA content in the *pps-1* mutant appears to affect the vegetative phase change. Certainly, GA<sub>3</sub> application promotes the vegetative phase change in this mutant, although it does not completely restore the normal phenotype. Accordingly, *PPS* seems to partially regulate the phase change by affecting the amount of GA, but it also controls phase change–specific pathways, such as those regulating *miR156/miR172* expression, independently of GA.

In spite of its prolonged juvenile phase, the *pps-1* mutant flowers early, indicating that its adult phase is shortened dramatically. This characteristic contrasts notably with the many heterochronic mutants of maize (Dudley and Poethig, 1993; Moose and Sisco, 1994; Evans and Poethig, 1995; Vega et al., 2002; Chuck et al., 2007), such as *Teopod1* (*Tp1*), *Tp2*, *Cg1*, and *dwarf1* (*d1*), that have a prolonged juvenile phase together with late flowering (Dudley and Poethig, 1993; Evans and Poethig, 1995; Chuck et al., 2007). In addition, the *gl15* and *early phase change* maize mutants, which have a shortened juvenile phase, exhibit flowering times comparable to or earlier than that of the wild-type plant (Moose and Sisco, 1994; Vega et al., 2002). Thus, the duration of the juvenile phase does not seem to greatly affect the duration of the adult phase in these maize mutants. In this context, *pps-1* is a unique heterochronic mutant.

The mechanism of early flowering in *pps-1* is interesting. Although most early flowering rice mutants or cultivars exhibit precocious activation of *Hd3a/RFT1* expression (Izawa et al., 2002; Kim et al., 2008; Andrés et al., 2009), *Hd3a/RFT1* expression is almost completely suppressed in the *pps-1* mutant, regardless of daylength. Instead, the mutant exhibits derepressed expression of *RAP1B*, which normally acts downstream of *Hd3a/RFT1* and may function in floral meristem and determine floral organ identity. It has been reported that ectopic expression



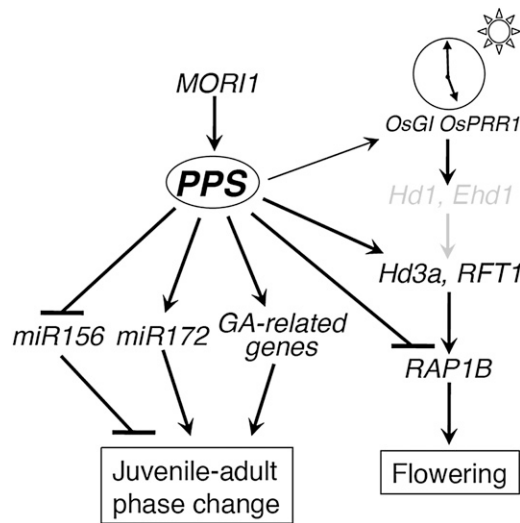


**Figure 8.** Schematic Representation of Gene Cascades Involved in Phase Changes in Rice.

*Hd1* and *EHD1* correspond to *CO* in *Arabidopsis*, and *Hd3a* and *RFT1* to *FT* in *Arabidopsis*. Note that *Hd1* and *Ehd1* are written in gray because Taichung 65, the background cultivar of *pps*, harbors mutant alleles of *Hd1* and *Ehd1*. Otherwise, they are written in black.

of *RAP1B* resulted in a drastic early flowering (Jeon et al., 2000). Therefore, *PPS* regulates flowering time by suppressing the expression of *RAP1B* (and possibly of other floral meristem identity genes) independent of the *Hd1-Ehd1-Hd3a/RFT1* pathway (Figure 8; Itoh et al., 2010).

One of the major functions of *Arabidopsis COP1* is repressing photomorphogenesis in the dark. In darkness, wild-type plants show elongated hypocotyls and unopened cotyledons, and mRNA levels of light-regulated genes such as *CAB* are strongly repressed (Deng et al., 1991). Conversely, dark-grown *cop1-1* exhibits light-grown characteristics at both morphological and mRNA levels (Deng et al., 1991). Similar phenotypes were observed in *pps-1* plants. The introduction of rice *COP1/PPS* into a *cop1* mutant complements the photomorphogenesis phenotype in the dark (Tsuge et al., 2001). Thus, *PPS* and *Arabidopsis COP1* have a conserved function: the repression of photomorphogenesis in the dark. This conclusion is supported by the fact that the *pps-1* mutant exhibits photomorphogenesis in dark conditions.

Although *PPS* is similar to *Arabidopsis COP1* in its photomorphogenesis-repressing function, *PPS* also appears to have functions that have not been reported for *COP1*. First, *PPS* promotes the vegetative phase change by regulating GA biosynthesis and *miR156/miR172* expression, whereas the effect of *COP1* on the vegetative phase change has not been reported. In fact, our analysis suggests that the timing of the juvenile–adult phase change is similar in wild-type and *cop1-4 Arabidopsis* plants. Second, *PPS* can control flowering time via the *Hd1*-independent pathway, since *Hd1* was mutated in both Taichung 65 and *pps* mutants. The *cop1* mutant exhibits a flowering time comparable to that of wild-type plants under long-day conditions

and earlier than that of wild-type plants under short-day conditions (McNellis et al., 1994), and *COP1* affects flowering time via the *CO-FT* pathway, mainly due to the control of CO protein degradation via *COP1/SPA1* system (Valverde et al., 2004; Laubinger et al., 2006; Jang et al., 2008; Liu et al., 2008; Chen et al., 2010). Thus, the mechanism by which *PPS* regulates flowering time is a unique one.

*PPS* has acquired important and opposing functions in two independent transitions: it promotes the juvenile–adult phase change and represses the vegetative–reproductive stage transition. By regulating several different genetic pathways, *PPS* performs an important biological function in plant development: it integrates the phase transitions. Although the functions of *Arabidopsis COP1* in vegetative development in the light have not yet been intensively analyzed, our results underscore the divergence of the downstream events controlled by *PPS/COP1* in different species.

We also characterized the temporal dynamics and sites of *PPS* expression. *PPS* expression is suppressed in juvenile leaves (i.e., leaves 1 and 2), begins to increase in third leaves, and reaches a maximum in fourth and fifth leaves, which are intermediate between the juvenile and adult leaves. This pattern indicates that *PPS* primarily regulates the onset of adult phase. The period of maximum *PPS* expression (Figure 5) coincides with the period of rapid change in *miR156* and *miR172* expression (Figure 2). Thus, we assume that *PPS* plays a role in triggering adult phase development downstream of *MOR11* and upstream of GA-related genes and miRNAs.

*PPS* is expressed at a much lower level in the shoot apex than in leaves, indicating that the juvenile–adult phase change is initiated primarily in the leaves and not in the shoot apex. This aspect of *PPS* expression implies that certain factors determining adult phase identity may initiate in the leaves. These factors must be translocated to the rest of the plant, as adult phase traits are observed not only in leaves but also in the SAM and stem. Similarly, the results of clonal analysis and apex culture of maize have suggested that the vegetative phase identity of a leaf is determined after leaf initiation and that the factors initiating phase change do not originate in the SAM (Orkiszewski and Poethig, 2000). A recent study also revealed that leaf-derived signal represses the *miR156* transcription to regulate vegetative phase change in *Arabidopsis* and *Nicotiana benthamiana* (Yang et al., 2011). The vegetative–reproductive phase change is regulated by the FT/*Hd3a* protein, known as florigen, which is produced in leaves and translocates to the SAM to transform it into an inflorescence meristem (Tamaki et al., 2007). If the first event of the vegetative phase change takes place in leaves, some signal must be transmitted from the leaves to the SAM and stem, as SAM size, node–internode differentiation, and structural phenotypes are phase specific. Further studies of *PPS*-dependent phase regulation might result in the identification of a florigen-like factor mediating the vegetative phase change in rice.

This study was conducted to reveal the role of the *PPS* gene in the cascade associated with the vegetative phase change in rice. We conclude that *PPS* triggers adult development downstream of *MOR11* and regulates the expression of downstream genes. It also regulates flowering time and thus might be a key gene, one that integrates phase changes during rice development (Figure 8).

## METHODS

### Plant Materials

Two single recessive allelic mutants, *pps-1* and *pps-2*, of rice (*Oryza sativa*) showing small seedlings with small leaves were identified from an M2 population of cv Taichung 65 mutagenized with *N*-methyl-*N*-nitrosourea. Taichung 65 was used as the wild type. We also used the *mori1-1* mutant reported previously (Asai et al., 2002), which perpetuates the juvenile phase and fails to become adult and also *d18-dy*, which is a dwarf mutant defective in the GA biosynthetic gene encoding GA3 OXIDASE2. Mutants and wild-type plants were grown in paddy fields or in pots under natural field conditions.

The *Arabidopsis thaliana cop1-4* mutant (McNellis et al., 1994) and its background ecotype Columbia were grown in a growth chamber under daily cycles of long-day (14 h light/10 h dark) conditions at 23°C.

### Paraffin Sectioning

Leaves and shoot apices were fixed with FAA (formalin:acetic acid:50% ethanol, 1:1:18) for 24 h at 4°C. They were dehydrated in a graded ethanol series and embedded in Paraplast plus (McCormick Scientific). Microtome sections (8 μm thick) were stained with Delafield's hematoxylin (Muto Pure Chemicals) and observed with a light microscope.

### Measurement of Photosynthetic Rate

For measuring photosynthesis, fully expanded second, fourth, sixth, eighth, and 10th leaves of the wild type and fourth, sixth, and eighth leaves of *pps-1* mutant were used. Rates of photosynthetic CO<sub>2</sub> assimilation were measured using a portable gas exchange system (LI-6400; Li-Cor). Measurements were made on intact leaf blades between 9 AM and noon and replicated for three plants. Light was provided by an LED source (red/blue, 6400-02 LED source; Li-Cor). During the measurement of photosynthetic CO<sub>2</sub> assimilation rates, the photon flux density was 1300 μmol photons m<sup>-2</sup> s<sup>-1</sup>, leaf temperature was 25°C, and the reference CO<sub>2</sub> concentration was 370 ppm.

### Gene Expression Profiling

Total RNA was extracted using TRIzol reagent (Invitrogen) from 10-d-old wild-type and *pps-1* seedlings under the light and dark conditions for *CAB* expression. For quantifying the *CAB* expression relative to *ACT1* expression, RT-PCR was performed using Super Script III (Invitrogen). The primers for *CAB* and *ACT1* are listed in Supplemental Table 1 online. We performed RT-PCR for appropriate cycles at 95°C for 30 s, 60°C for 30 s, and 72°C for 20 s.

To monitor *PPS* expression, total RNA was extracted using the High Capacity RNA-to-cDNA Master Mix (Applied Biosystems) from wild-type second, third, fourth, fifth, sixth, and seventh leaves. To quantify the *PPS* expression relative to *ACT1* expression, PCR was performed using the TaqMan Fast Universal PCR Master Mix, FAM-labeled TaqMan probes for each gene (Applied Biosystems), and the StepOnePlus real-time PCR system (Applied Biosystem). The expression level of each sample was normalized against that of an internal control, *ACT1*. The primers and probes for *ACT1* and *PPS* are listed in Supplemental Table 1 online. All TaqMan probes except *ACT1* probe include FAM dye at the 5'-end and TAMRA at the 3'-end. *ACT1* probe includes FAM dye at the 5'-end and BHQ at the 3'-end.

The real-time PCR for *miR156* and *miR172* was performed using TaqMan MicroRNA assay (Applied Biosystems). We used the same wild-type leaves as used for *PPS* expression. In addition, RNA was also isolated from *pps-1* second, third, fourth, fifth, sixth, and seventh leaves.

For *miR156* and *miR172* expression assay in *Arabidopsis*, total RNA was extracted using TRIzol reagent (Invitrogen) from 10-d-old Columbia and *cop1-4* whole seedlings. The real-time PCR for *miR156* and *miR172* was performed using TaqMan MicroRNA assay. We used *ACTIN-2* as an internal control, and quantitative PCR was conducted using SYBR green master mix (Applied Biosystems). The primers for *ACTIN-2* are listed in Supplemental Table 1 online. For GA metabolic gene expression, total RNA was isolated from wild-type and *pps-1* fourth leaves. The primers and probes for *GA2ox4*, *GA3ox2*, and *GA20ox2* are listed in Supplemental Table 1 online.

For expression analysis of flowering time genes (*Hd3a*, *RFT*, and *RAP1B/Os MADS14*), wild-type and *pps-1* seeds were imbibed in darkness (48 h at 30°C) and then sown in soil. Plants were grown in a growth chamber at 70% humidity under daily cycles of short-day (10 h light/14 h dark) or long-day (14.5 h light/9.5 h dark) conditions at 28°C in the light and 24°C in the dark. Light was applied by a metal halide lamp (photosynthetic photon flux density 450 μmol per m<sup>2</sup> per s). Flowering time was counted as the time when the first panicle emerged. Total RNA was extracted from leaves of 14-d-old seedlings using an RNeasy Plant Mini Kit (Qiagen) in accordance with the manufacturer's instructions. First-strand cDNA was synthesized from 5 mg of total RNA using Superscript II reverse transcriptase (Invitrogen). Real-time quantitative RT-PCR was performed using the Taq-Man PCR method on an ABI PRISM 7900 sequence detection system, as described previously (Ogiso et al., 2010). Gene-specific primers and probes for *Hd3a*, *RFT*, *RAP1B*, and *UBQ* are listed in Supplemental Table 1 online.

### Measurement of GA Content and GA<sub>3</sub> Application

For measuring GA content, sampling of ~100 mg of 3-week-old seedlings from more than five plants was repeated three times for *pps-1* and the wild type, respectively. Extraction and determination of GA for each sample were performed using a liquid chromatography-tandem mass spectrometry system (AQUITY UPLC/Quattro Premier) as described previously (Kojima et al., 2009).

For observing responses to GA, sterilized seeds of *pps-1* and the wild type were plated on Murashige and Skoog (1962) medium containing 10<sup>-5</sup> M GA<sub>3</sub> (Sigma-Aldrich) or 10<sup>-5</sup> M uniconazole P (Wako). Plants were grown in a growth chamber under the continuous light at 28°C.

### Map-Based Cloning

To map the *PPS* locus, *pps-1* heterozygous plant was crossed with cv Kasalath (*ssp indica*). Using mutant plants segregated in the F<sub>2</sub> population, *PPS* locus was roughly mapped on the long arm of chromosome 2. Further mapping limited the *PPS* locus around 139.5 centimorgans between one cleaved-amplified polymorphic sequence marker and one sequence-tagged sites marker. These two closest markers are listed in Supplemental Table 1 online. The genomic sequence of *PPS* (LOC\_Os02g53140 in TIGR) in *pps-1* was amplified by PCR using ExTaq DNA polymerase (TaKaRa). The amplified PCR products were directly sequenced using a dye terminator cycle sequencing kit and an ABI PRISM 310 sequencer (Applied Biosystems).

### Expression of Circadian Clock-Related Genes, *GI*, *PRR1*, and *LHY*

Wild-type and *pps-1* plants were entrained under short-day conditions for 14 d. Then, samples were collected at every 3 h. Total RNA was extracted using the RNeasy plant mini kit (Qiagen). cDNA was synthesized using SuperscriptII RTase (Invitrogen). Real-time quantitative PCR was performed by Taq-Man PCR method on an ABI PRISM 7900 sequence detection system. Primers and probes for rice (*Os*) *GI*, *PRR1*, and *LHY* are listed in Supplemental Table 1 online.

### Detection of PPS Transcripts and Amino Acid Alignment of COP1 Orthologs

Total RNA was extracted using TRIzol reagent (Invitrogen) from wild-type and *pps-1* 1-week-old seedlings. RT-PCR was performed using Super Script III (Invitrogen). The primers are listed in Supplemental Table 1 online. We performed RT-PCR for appropriate cycles at 95°C for 30 s, 60°C for 30 s, and 72°C for 20 s. The amino acid sequences of two genes that have the highest homology with PPS in maize and *Arabidopsis* were selected by BLAST research (National Center for Biotechnology Information; <http://www.ncbi.nlm.nih.gov/>).

### Complementation Test

PPS cDNA was inserted into a binary vector containing the rice *ACT1N* promoter and nos terminator (*pACT:PPS*) and was introduced into the *pps-1* homozygous calli using the *Agrobacterium tumefaciens*-mediated transformation method (Hiei et al., 1994). The primers for full-length PPS cDNA amplification are listed in Supplemental Table 1 online.

### Tissue-Specific Expression Pattern of PPS

To examine PPS expression, total RNA was extracted using TRIzol reagent (Invitrogen) from wild-type fourth leaf of 1-week-old shoot apex, 3-week-old shoot apex, 5-week-old shoot apex, young panicle at primary rachis branch differentiation stage, young panicle at secondary rachis branch differentiation stage, and young panicle at floral organ differentiation stage. RT-PCR was performed using Super Script III (Invitrogen). The primers are listed in Supplemental Table 1 online. We performed quantitative RT-PCR for appropriate cycles at 95°C for 30 s, 60°C for 30 s, and 72°C for 20 s.

### Accession Numbers

Sequence data from this article can be found in the GenBank/EMBL database or the Arabidopsis Genome Initiative database under the following accession numbers: AB634500 (*PPS*), AK058305 (*CAB*), AK058421 (*ACT1*), AK101713 (*GA2ox4*) AB056518 (*GA3ox2*), AB077025 (*GA2ox2*), AB052943 (*Hd3a*), AB062676 (*RFT1*), AK121171 (*RAP1B*), AK101547 (*UBQ*), AK072166 (*Os Gl*), AK111828 (*Os PRR1*), AK111893 (*Os LHY1*), NP\_188508 (*ACT2*), and NM 128855 (*COP1*).

### Supplemental Data

The following materials are available in the online version of this article.

**Supplemental Figure 1.** Circadian Clock-Related Gene Expression under Short-Day Conditions.

**Supplemental Figure 2.** Detection of PPS Transcripts.

**Supplemental Figure 3.** Complementation Test of *pps-1*.

**Supplemental Figure 4.** RT-PCR Analysis of PPS Expression.

**Supplemental Table 1.** List of Primers Used in This Study.

### ACKNOWLEDGMENTS

We thank T. Tsuge (Kyoto University) for kind gift of *cop1-4* seeds. We also thank R. Soga and K. Ichikawa (University of Tokyo) for their assistance in cultivating rice plants at the Experimental Farm of the University of Tokyo. This work is supported in part by a Grant-in-Aid for Scientific Research from the Ministry of Education, Culture, Sports, Science and Technology of Japan (20248001 and 23658005 to Y.N.).

### AUTHOR CONTRIBUTIONS

N.T., J.-I.I., and Y.N. designed the experiments. N.T. performed most experiments. M.K. and H.S. measured GA content. N.S. measured photosynthetic rate. H.I. and T.I. performed experiments on flowering time-related gene expression. N.T., J.-I.I., and Y.N. wrote the article.

Received January 25, 2011; revised May 10, 2011; accepted June 11, 2011; published June 24, 2011.

### REFERENCES

- Alabadí, D., Gallego-Bartolomé, J., Orlando, L., García-Cárcel, L., Rubio, V., Martínez, C., Frigerio, M., Iglesias-Pedraz, J.M., Espinosa, A., Deng, X.W., and Blázquez, M.A. (2008). Gibberellins modulate light signaling pathways to prevent *Arabidopsis* seedling de-etioliation in darkness. *Plant J.* **53**: 324–335.
- Andrés, F., Galbraith, D.W., Talón, M., and Domingo, C. (2009). Analysis of *PHOTOPERIOD SENSITIVITY5* sheds light on the role of phytochromes in photoperiodic flowering in rice. *Plant Physiol.* **151**: 681–690.
- Asai, K., Satoh, N., Sasaki, H., Satoh, H., and Nagato, Y. (2002). A rice heterochronic mutant, *mori1*, is defective in the juvenile-adult phase change. *Development* **129**: 265–273.
- Aukerman, M.J., and Sakai, H. (2003). Regulation of flowering time and floral organ identity by a microRNA and its *APETALA2*-like target genes. *Plant Cell* **15**: 2730–2741.
- Chen, H., Huang, X., Gusmaroli, G., Terzaghi, W., Lau, O.S., Yanagawa, Y., Zhang, Y., Li, J., Lee, J.H., Zhu, D., and Deng, X.W. (2010). *Arabidopsis* CULLIN4-damaged DNA binding protein 1 interacts with CONSTITUTIVELY PHOTOMORPHOGENIC1-SUPPRESSOR OF PHYA complexes to regulate photomorphogenesis and flowering time. *Plant Cell* **22**: 108–123.
- Chuck, G., Cigan, A.M., Saetern, K., and Hake, S. (2007). The heterochronic maize mutant *Corngrass1* results from overexpression of a tandem microRNA. *Nat. Genet.* **39**: 544–549.
- Deng, X.W., Caspar, T., and Quail, P.H. (1991). *cop1*: A regulatory locus involved in light-controlled development and gene expression in *Arabidopsis*. *Genes Dev.* **5**: 1172–1182.
- Doi, K., Izawa, T., Fuse, T., Yamanouchi, U., Kubo, T., Shimatani, Z., Yano, M., and Yoshimura, A. (2004). Ehd1, a B-type response regulator in rice, confers short-day promotion of flowering and controls *FT*-like gene expression independently of *Hd1*. *Genes Dev.* **18**: 926–936.
- Dudley, M., and Poethig, R.S. (1993). The heterochronic *Teopod1* and *Teopod2* mutations of maize are expressed non-cell-autonomously. *Genetics* **133**: 389–399.
- Evans, M.M., and Poethig, R.S. (1995). Gibberellins promote vegetative phase change and reproductive maturity in maize. *Plant Physiol.* **108**: 475–487.
- Hiei, Y., Ohta, S., Komari, T., and Kumashiro, T. (1994). Efficient transformation of rice (*Oryza sativa* L.) mediated by *Agrobacterium* and sequence analysis of the boundaries of the T-DNA. *Plant J.* **6**: 271–282.
- Hunter, C., Sun, H., and Poethig, R.S. (2003). The *Arabidopsis* heterochronic gene *ZIPPY* is an ARGONAUTE family member. *Genes Dev.* **18**: 2368–2379.
- Itoh, J., Nonomura, K., Ikeda, K., Yamaki, S., Inukai, Y., Yamagishi, H., Kitano, H., and Nagato, Y. (2005). Rice plant development: From zygote to spikelet. *Plant Cell Physiol.* **46**: 23–47.
- Itoh, H., Nonoue, Y., Yano, M., and Izawa, T. (2010). A pair of floral

- regulators sets critical day length for Hd3a florigen expression in rice. *Nat. Genet.* **42**: 635–638.
- Izawa, T., Oikawa, T., Sugiyama, N., Tanisaka, T., Yano, M., and Shimamoto, K.** (2002). Phytochrome mediates the external light signal to repress *FT* orthologs in photoperiodic flowering of rice. *Genes Dev.* **16**: 2006–2020.
- Jang, S., Marchal, V., Panigrahi, K.C., Wenkel, S., Soppe, W., Deng, X.W., Valverde, F., and Coupland, G.** (2008). *Arabidopsis COP1* shapes the temporal pattern of CO accumulation conferring a photoperiodic flowering response. *EMBO J.* **27**: 1277–1288.
- Jaya, E., Kubien, D.S., Jameson, P.E., and Clemens, J.** (2010). Vegetative phase change and photosynthesis in *Eucalyptus occidentalis*: Architectural simplification prolongs juvenile traits. *Tree Physiol.* **30**: 393–403.
- Jeon, J.-S., Lee, S., Jung, K.-H., Yang, W.-S., Yi, G.-H., Oh, B.-G., and An, G.** (2000). Production of transgenic rice plants showing reduced heading date and plant height by ectopic expression of rice MADS-box genes. *Mol. Breed.* **6**: 581–592.
- Kim, S.K., Yun, C.H., Lee, J.H., Jang, Y.H., Park, H.Y., and Kim, J.K.** (2008). *OsCO3*, a *CONSTANS*-LIKE gene, controls flowering by negatively regulating the expression of *FT*-like genes under SD conditions in rice. *Planta* **228**: 355–365.
- Kojima, M., Kamada-Nobusada, T., Komatsu, H., Takei, K., Kuroha, T., Mizutani, M., Ashikari, M., Ueguchi-Tanaka, M., Matsuoka, M., Suzuki, K., and Sakakibara, H.** (2009). Highly sensitive and high-throughput analysis of plant hormones using MS-probe modification and liquid chromatography-tandem mass spectrometry: An application for hormone profiling in *Oryza sativa*. *Plant Cell Physiol.* **50**: 1201–1214.
- Komiya, R., Ikegami, A., Tamaki, S., Yokoi, S., and Shimamoto, K.** (2008). *Hd3a* and *RFT1* are essential for flowering in rice. *Development* **135**: 767–774.
- Laubinger, S., Marchal, V., Le Gourrierec, J., Wenkel, S., Adrian, J., Jang, S., Kulajta, C., Braun, H., Coupland, G., and Hoecker, U.** (2006). *Arabidopsis* SPA proteins regulate photoperiodic flowering and interact with the floral inducer *CONSTANS* to regulate its stability. *Development* **133**: 3213–3222. Erratum. *Development* **133**: 4608.
- Lauter, N., Kampani, A., Carlson, S., Goebel, M., and Moose, S.P.** (2005). *microRNA172* down-regulates *glossy15* to promote vegetative phase change in maize. *Proc. Natl. Acad. Sci. USA* **102**: 9412–9417.
- Lawson, E.J., and Poethig, R.S.** (1995). Shoot development in plants: Time for a change. *Trends Genet.* **11**: 263–268.
- Liu, L.J., Zhang, Y.C., Li, Q.H., Sang, Y., Mao, J., Lian, H.L., Wang, L., and Yang, H.Q.** (2008). COP1-mediated ubiquitination of *CONSTANS* is implicated in cryptochrome regulation of flowering in *Arabidopsis*. *Plant Cell* **20**: 292–306.
- McNellis, T.W., von Arnim, A.G., Araki, T., Komeda, Y., Miséra, S., and Deng, X.W.** (1994). Genetic and molecular analysis of an allelic series of *cop1* mutants suggests functional roles for the multiple protein domains. *Plant Cell* **6**: 487–500.
- Millar, A.J., Straume, M., Chory, J., Chua, N.H., and Kay, S.A.** (1995). The regulation of circadian period by phototransduction pathways in *Arabidopsis*. *Science* **267**: 1163–1166.
- Moose, S.P., and Sisco, P.H.** (1994). *Glossy15* controls the epidermal juvenile-to-adult phase transition in maize. *Plant Cell* **6**: 1343–1355.
- Moose, S.P., and Sisco, P.H.** (1996). *Glossy15*, an *APETALA2*-like gene from maize that regulates leaf epidermal cell identity. *Genes Dev.* **10**: 3018–3027.
- Murashige, T., and Skoog, F.** (1962). A revised medium for rapid growth and bioassays with tobacco tissue cultures. *Physiol. Plant.* **15**: 473–497.
- Ogiso, E., Takahashi, Y., Sasaki, T., Yano, M., and Izawa, T.** (2010). The role of casein kinase II in flowering time regulation has diversified during evolution. *Plant Physiol.* **152**: 808–820.
- Orkiszewski, J.A., and Poethig, R.S.** (2000). Phase identity of the maize leaf is determined after leaf initiation. *Proc. Natl. Acad. Sci. USA* **97**: 10631–10636.
- Peragine, A., Yoshikawa, M., Wu, G., Albrecht, H.L., and Poethig, R.S.** (2004). *SGS3* and *SGS2/SDE1/RDR6* are required for juvenile development and the production of trans-acting siRNAs in *Arabidopsis*. *Genes Dev.* **18**: 2368–2379.
- Poethig, R.S.** (1990). Phase change and the regulation of shoot morphogenesis in plants. *Science* **250**: 923–930.
- Poethig, R.S.** (2003). Phase change and the regulation of developmental timing in plants. *Science* **301**: 334–336.
- Schwab, R., Palatnik, J.F., Riester, M., Schommer, C., Schmid, M., and Weigel, D.** (2005). Specific effects of microRNAs on the plant transcriptome. *Dev. Cell* **8**: 517–527.
- Schwarz, S., Grande, A.V., Bujdosó, N., Saedler, H., and Huijser, P.** (2008). The microRNA regulated SBP-box genes *SPL9* and *SPL15* control shoot maturation in *Arabidopsis*. *Plant Mol. Biol.* **67**: 183–195.
- Simpson, G.G., Gendall, A.R., and Dean, C.** (1999). When to switch to flowering. *Annu. Rev. Cell Dev. Biol.* **15**: 519–550.
- Smith, M.R., Willmann, M.R., Wu, G., Berardini, T.Z., Möller, B., Weijers, D., and Poethig, R.S.** (2009). *Cyclophilin 40* is required for microRNA activity in *Arabidopsis*. *Proc. Natl. Acad. Sci. USA* **106**: 5424–5429.
- Tamaki, S., Matsuo, S., Wong, H.L., Yokoi, S., and Shimamoto, K.** (2007). Hd3a protein is a mobile flowering signal in rice. *Science* **316**: 1033–1036.
- Telfer, A., Bollman, K.M., and Poethig, R.S.** (1997). Phase change and the regulation of trichome distribution in *Arabidopsis thaliana*. *Development* **124**: 645–654.
- Telfer, A., and Poethig, R.S.** (1998). *HASTY*: A gene that regulates the timing of shoot maturation in *Arabidopsis thaliana*. *Development* **125**: 1889–1898.
- Tsuge, T., Inagaki, N., Yoshizumi, T., Shimada, H., Kawamoto, T., Matsuzaki, R., Yamamoto, N., and Matsui, M.** (2001). Phytochrome-mediated control of *COP1* gene expression in rice plants. *Mol. Genet. Genomics* **265**: 43–50.
- Valverde, F., Mouradov, A., Soppe, W., Ravenscroft, D., Samach, A., and Coupland, G.** (2004). Photoreceptor regulation of *CONSTANS* protein in photoperiodic flowering. *Science* **303**: 1003–1006.
- Vega, S.H., Sauer, M., Orkiszewski, J.A., and Poethig, R.S.** (2002). The early phase change gene in maize. *Plant Cell* **14**: 133–147.
- Weller, J.L., Hecht, V., Vander Schoor, J.K., Davidson, S.E., and Ross, J.J.** (2009). Light regulation of gibberellin biosynthesis in pea is mediated through the *COP1/HY5* pathway. *Plant Cell* **21**: 800–813.
- Wu, G., Park, M.Y., Conway, S.R., Wang, J.W., Weigel, D., and Poethig, R.S.** (2009). The sequential action of *miR156* and *miR172* regulates developmental timing in *Arabidopsis*. *Cell* **138**: 750–759.
- Wu, G., and Poethig, R.S.** (2006). Temporal regulation of shoot development in *Arabidopsis thaliana* by *miR156* and its target *SPL3*. *Development* **133**: 3539–3547.
- Yang, L., Conway, S.R., and Poethig, R.S.** (2011). Vegetative phase change is mediated by a leaf-derived signal that represses the transcription of *miR156*. *Development* **138**: 245–249.